Spectral Efficiency of Massive MIMO using FBMC-OQAM Modulation

Felipe Kurpiel Jose, Luis Lolis, Eduardo Parente Ribeiro and Felipe Alex Pinto

***Abstract*— This article covers the potential of Filter Bank Multicarrier (FBMC) modulation to be used in the future 5G wireless networks where Massive Multiple-Input Multiple-Output (MIMO) will be deployed. The study compares orthogonal frequency division multiplexing (OFDM) with FBMC. The former is the multiplexing technique in 4G communications and the latter is one of the strongest candidates to replace OFDM in 5G networks. This comparison evaluates the spectral efficiency (SE) of a massive MIMO (MM) system uplink under a single-cell environment. Due to the absence of the cyclic prefix, the FBMC has better SE than the OFDM as the signal-to-noise-ratio (SNR) increases. However, to the best of the authors' knowledge, this study has not yet been conducted under a MM scenario. In summary, this article presents an analysis of SE of FBMC considering a MM setup. While limiting the modulation to 64-Quadrature Amplitude Modulation (QAM) per sub carrier, it was observed that as the SE increases, the required number of antennas for the OFDM becomes the double or the triple of the counterpart using FBMC, or even it is not achieved by the OFDM.**

***Keywords*— Massive MIMO, FBMC, M-QAM modulation, spectral efficiency, 5G**

I. Introduction

The traffic of wireless communication networks has grown exponentially and transmission rates are nearing 1 Gb/s nowadays, which leads to higher demands on system capacity. Moreover, designing wireless links with superior speed, quality-of-service and capability represents a significant engineering and research challenge. [1]

Multiple-input multiple-output (MIMO) systems have emerged to serve tens of user equipment (UE) by employing hundreds of base station (BS) antennas in the same time-frequency resource. As a definition, Massive MIMO (MM) is a multi-user MIMO technology where a number K of UE antennas are serviced on the same time-frequency resource by a BS with M antennas such that M >> K. In reality, MM has become the strongest candidate to increase the capacity of multiuser networks [2].

Many studies analyses the spectral efficiency (SE) of MM under different scenarios [3]–[5]. In all of them, the orthogonal frequency division multiplexing (OFDM) is adopted as the multiplexing / modulation scheme. It is important to point out that all these studies considered that each sub-carrier has a Gaussian distributed modulation, being that a condition to achieve the Shannon limit per channel [6].

Felipe Kurpiel Jose, Luis Lolis, Eduardo Parente Ribeiro and Felipe Alex Pinto. Federal University of Parana (UFPR), Curitiba-PR, Brazil, E-mails: lipekurpiel@gmail.com, luis.lolis@eletrica.ufpr.br, edu@ufpr.br, felipe.fap.ufpr@gmail.com. This work was partially supported by UFPR.

As explained in [7], every existent waveform have its pros and cons, hence the benefits of large antenna arrays can turn a MM specific waveform combination more attractive than others. Compared to existing 4G technologies, 5G is targeting much higher throughput with sub-ms latency and utilizing higher carrier frequencies and wider bandwidths [8]. Given that, the filter bank multicarrier (FBMC) represents a possibility to provide higher SE and it is much more suited to a potential 5G system than OFDM [9].

In [10], the OFDM and FBMC SEs are compared with the theoretical bounds for Rayleigh fading and a single-input single-output (SISO) transmission. Each sub-carrier changed between M-QAM going from $M = 4$ to $M = 64$. In addition, block error-correcting codes having rates from 78/1024 to 948/1024 were also applied. The SNR for a specific throughput is achieved when the bit error rate (BER) around 10^{-3}, which is obtained through Monte-Carlo simulations.

This paper presents an SE analysis for the OFDM and FBMC modulation / multiplexing schemes for MM cells, combining the work in [10], [3] and [4]. The individual SE per SNR from [10] is applied in the averaged perceived SNR per user obtained in [3] and [4] in a MM cell, to evaluate the SE in the entire cell, with different number of antennas and cell size. By adopting this strategy, the modulations being considered in a single-cell environment on a MM system uplink are presented in a more realistic format. In other words, the FBMC and OFDM sub-carriers are not seen as Gaussian distributions. In summary, this approach provides a more realistic scenario for the analysis of SE in a MM system uplink than what is presented on both [3] and [4].

The remainder of this paper is organized as follows: Section II provides the theoretical framework for MM and FBMC. In Section III the method to analyze non-Gaussian modulations is described. In Section IV the SE for FBMC and OFDM in MM is presented. In Section V the numerical results are provided and insightful discussions are drawn. Finally, Section VI concludes the paper.

II. Theoretical Framework

A. Uplink Massive MIMO

The design and analysis of MIMO systems includes one BS equipped with an array of M antennas that receive data from K single-antenna users. In [3] the SE of a MIMO system uplink for a single cell environment is evaluated considering lower capacity bounds in a channel model that includes small-scale fading. The study focus on three different linear detectors at the BS: maximum-ratio combining (MRC), zero-forcing (ZF) and minimum-mean-square error (MMSE) detection. In addition, each user is uniformly distributed inside a single circular cell of radius R where a Monte Carlo simulation places the users to validate the study. In this case, the individual UE is linked to an average perceived SNR value.

According to [3], when the ZF Receiver is employed, the uplink rate for the k^{th} user under Rayleigh fading channel with noise variance equal to 1, and provided that $M \geq K+1$, the achievable uplink rate for the k^{th} user is lower bounded by:

$$SE_{ZF} = \log_2[1 + (M-K)p_u\beta_k]. \tag{1}$$

where β_k is the small-scale fading for the k^{th} user, p_u is the average transmitted power of each user. The cell SE is defined as:

$$SE_{ZF_{cell}} = \sum_{k=1}^{K} \log_2[1 + (M-K)p_u\beta_k]. \tag{2}$$

Similarly, the SE for the MM system uplink in a single-cell environment is analyzed in [4], where K single UE antennas send signals to one of the M antennas at BS. An analytic expression for SE is derived by employing the MRC and ZF detection at the BS. Those authors considered a flat-fading Rayleigh MIMO channel for each subcarrier, besides subcarrier modulated signal is considered Gaussian distributed. It is also considered that perfect channel state information (CSI) can be acquired at the BS when UEs send pilot sequences in the uplink. With perfect CSI, a power control is introduced in order to vary p_u leading to a single SNR for all users. The expected SNR is analytically derived. First a large scale fading is introduced:

$$\beta_{k(large)} = \frac{\phi\xi_k}{d_k^\alpha}, \tag{3}$$

where d_k represents the path loss depending on the distance between the BS and the k^{th} UE and the loss exponent α, ϕ is a constant related to the antenna gain and the carrier frequency, α is the path-loss exponent, and ξ_k represents a lognormal distributed shadow fading variable:

$$10\log_{10}\xi_k \approx N(0, \sigma_{sh}^2); \tag{4}$$

then the analysis proceeds by finding the expected value for d_k^α and ξ_k:

$$E[d_k{}^\alpha] = \frac{2}{\alpha+2}\frac{R^{\ \alpha+2} - r_0^{\alpha+2}}{R^2 - r_0^2}, \tag{5}$$

$$E[\xi_k] = \left(\exp\left[\frac{1}{2}\left(\frac{ln10}{10}\sigma_{sh}\right)^2\right]\right)^{-1}, \tag{6}$$

where R is the cell radius, r_0 is the minimum distance between the UE and the BS. This leads to the average gain β in the cell:

$$\beta = E[\beta_k] = \frac{\phi E[\xi_k]}{E[d_k^\alpha]} \tag{7}$$

Once the power control is in place, an optimization is derived to relate the system Energy Efficiency (EE) and the SE. The system noise power spectrum density is no longer considered unitary, and is denoted by σ^2. A gain λ_o is derived to compensate the different losses and the cell power consumption in an optimal EE point. It is dependent on β, therefore, dependent on the cell size, and some other parameters such M, K, and variables related to the cell power consumption. In this case, every user experience the same SNR, optimized for EE. In this new scenario and considering ZF detection at the BS, the SE of a single user in a MM-OFDM system uplink can be approximated as:

$$SE_{ZF_o} = \log_2\left[1 + (M-K)\frac{\lambda_0}{\sigma^2}\right], \tag{8}$$

and the cell SE is defined by:

$$SE_{ZF_{o-cell}} = K\log_2\left[1 + (M-K)\frac{\lambda_0}{\sigma^2}\right], \tag{9}$$

It is evidenced in both (2) and (9) that the OFDM modulation is considered to be Gaussian distributed. According to [11], when the number of BS antennas tends to infinity, the processing gain of the system tends to infinity and, as a result, the effects of both noise and multiuser interference are completely eliminated. Furthermore, in order to deploy a large number of antennas at the BS it is reasonable to assume a scenario called favorable propagation. This case is described as a phenomenon observed when the wireless channel becomes near-deterministic and the BS-to-UE radio links become near-orthogonal to each other [12]. By adopting this assumption, the effects of small-scale fading, intra-cell interference and uncorrelated noise disappear asymptotically when M is sufficiently large. In addition, by using a linear detector as the ZF, the received signal is separated into streams which makes it possible to determine the received vector. Therefore, interference between terminals can be suppressed even further by using ZF [13].

B. *OFDM vs FBMC*

In essence, it is not expected to increase performance gains by 10 times when switching from OFDM to alternative schemes; still it is important to investigate viable candidates. It is known that the benefits of having large antenna arrays can turn a MM specific waveform combination more attractive than others [14]. FBMC for instance, offers lower out-of-band (OOB) emissions, and allows more affordable and more adaptable carrier aggregation than OFDM [15]. Still, by scaling up the number of antennas, the combination of MM and FBMC can offer benefits in several aspects including higher gains and better spectral efficiency if compared to OFDM [7].

As seen on [16], one of the most critical challenges on adopting FBMC instead of OFDM is in how to incorporate a multicarrier system based on filter banks to replace a conventional modulation scheme. In FBMC the Inverse Fast Fourier Transform (IFFT) plus Cyclic Prefix (CP) presented in the input of OFDM are replaced by a synthesis filter bank (SFB). When it comes to the output, the CP plus Fast Fourier Transform (FFT) of a OFDM system are replaced by the analysis filter bank (AFB). Synchronization is dealt when a sub-carrier is down-converted and the preamble is compared through correlation.

Due to the rectangular windowing, OFDM has strong sidelobes which is not the case of FBMC. By using filter banks, the energy is concentrated within the frequency range of a single subcarrier. According to [17], there is no need of guard bands in a FBMC scheme. Besides, carrier frequency offset (CFO) and inter carrier interference (ICI) due to Doppler Effect are almost eliminated.

Although the filter bank itself is slightly more complex than the respective element in OFDM, from a conceptual point of view, the signal generation in FBMC-offset quadrature amplitude modulation (FBMC-OQAM) and windowed OFDM requires basically the same operations. In summary, FBMC-OQAM can reuse many hardware components of OFDM [10].

In the comparison of OQAM versus QAM for non-orthogonal waveforms, OQAM can offer lower peak-to-average power ratio (PAPR), while smaller frame error rates (FERs) can be achieved by QAM in rich multipath fading channels. Moreover, FBMC adopts linear filtering to significantly reduce out-of-band (OOB) emission for the sake of SE and robustness against synchronization errors [18].

Taking all these details in mind, in [10] are presented real-world testbed measurements at 2.5GHz that are essential for this document. Under conditions that resemble a SISO signal with 1.4MHz LTE, it was demonstrated that FBMC has a higher throughput when compared to OFDM. This better performance is possible due to a higher usable bandwidth and because no CP is used on FBMC.

In this paper, OFDM is compared to FBMC in terms of spectral properties. Fig. 1 brings the simulated SE (considering perfect CSI for both modulations) and the theoretical bounds for Rayleigh fading as presented in [10]; where in the "FBMC Gaussian" each sub-carrier is a Gaussian distributed signal. The modulation scheme per sub-carrier varies from 4-QAM to 64-QAM. Block codes are added and combined with the modulation schemes, which gives a range of attainable SEs for different SNR values. Monte Carlo simulations are carried out an the Packet Error Rate (PER) is observed. The simulation goes until a PER of 10^{-3} is observed, then the modulation-coding scheme is changed.

As the SNR increases, the throughput for FBMC becomes higher compared to OFDM since it presents higher usable bandwidth and no CP. When compared to the Shannon limit, a critical note is that the SE saturates at 5 bits/s/Hz per user (from 64-QAM). Many challenges associated with FBMC were dealt with and validated by the real-world testbed measurements provided by [10]. In this work, the SE from these two modulation schemes is extended in the case of MM cell, with ZF signal combination.

III. SE for Non-Gaussian Modulations under SISO

FBMC presents superior spectral properties than OFDM, which is explored on this paper. In order to extract the SE based on real-world testbed measurements under a SISO signal, from the throughput data provided by [10], the bandwidth value must be known. With this in mind and knowing that both OFDM and FBMC are using the same 1.4MHz LTE bandwidth, it is straightforward to extract the curves for SE related to a SISO signal shown on Fig. 1.

By adopting Monte Carlo simulations it is possible to study the behavior of OFDM and FBMC modulation when both are

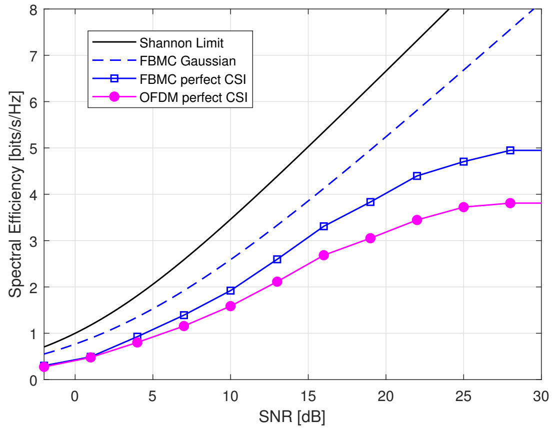

Fig. 1. Differences between FBMC and OFDM provided by real-world testbed measurements at 2.5GHz in a SISO signal, assuming perfect CSI.

not seen as Gaussian distributions. In other words, when the SE for different modulation schemes cannot be evaluated by theoretical models that follow the Shannon limit capacity [6]:

$$SE = \log_2[1 + SNR]. \tag{10}$$

Thus, there is a requirement to include a modulation element on the general formula of SE and by doing so, address the differences in performances shown on simulations when the modulations do not follow a Gaussian distribution. The SE for the OFDM and FBMC can be approximated to the Shannon limit by introduction a correction factor θ:

$$SE_{OFDM} = \log_2\left[1 + SNR \cdot |\theta_O|^2\right] \cdot \gamma_O \theta_O, \tag{11}$$

$$SE_{FBMC} = \log_2[1 + SNR \cdot |\theta_F|^2] \cdot \gamma_F \theta_F \tag{12}$$

where γ_O, γ_F, θ_O and θ_F are both SE correction factors for the OFDM and FBMC, respectively. The parameters γ_O and γ_F are constants, while θ varies with the SNR. The approximation is carried out as follows: for each SNR, the modulation SE is compared to the Shannon SE, then θ is obtained. Fig. 2 displays the curves related to the parameter of modulation $\theta \times \gamma$ vs SNR, under perfect CSI, of a SISO system; it illustrates that the difference between SE for OFDM and the Shannon limit is higher than what is seen when comparing FBMC. The correction factor γ is employed to adjust the point of saturation observed on simulation; its value is obtained through successive iterations until the curve fitting presents adherence. As γ is a constant, one can observe that θ by itself presents a close to linear behavior and therefore, it can be approximated to a linear equation. By assuming that, this new modulation factor has linear behavior, and knowing that there is a correlation between SE and SNR, the expression that represents the SE for non-Gaussian modulations (considering γ_O and γ_F constants related to OFDM and FBMC respectively) can be written as follows:

$$SE_{OFDM} = \log_2\left[1 + SNR\,|A_O SNR + B_O|^2\right] \gamma_O \cdot (A_O SNR + B_O) \tag{13}$$

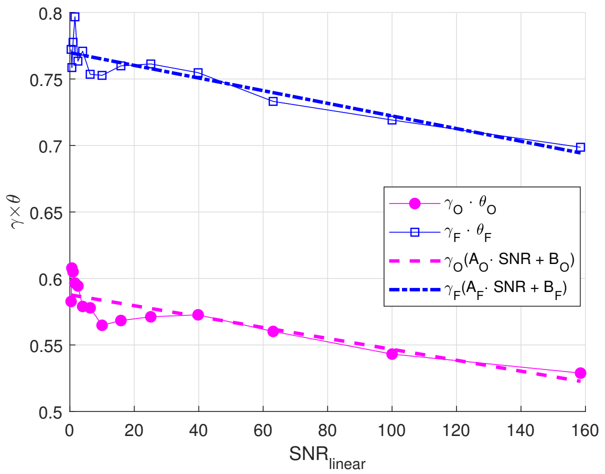

Fig. 2. Parameters $\theta \times \gamma$ versus SNR (linear) in SISO signal

$$SE_{FBMC} = \log_2 \left[1 + SNR \left| A_F SNR + B_F \right|^2 \right] \gamma_F \cdot (A_F SNR + B_F) \quad (14)$$

Table I shows the obtained parameter values for curve fitting. Comparatively, Fig. 3 show the close matching achieved between the modeling of (13) and (14) and the simulation results. The curve fitting is just part of the solution. The perceived SNR value for each user in a MM cell is used as reference to define SE for a single user and then multiplied per the number of users in the cell.

TABLE I
SE CORRECTION FACTORS FOR CURVE FITTING

	Parameters		
	A	B	γ
OFDM	-6×10^{-4}	0.8	0.75
FBMC	-5×10^{-4}	0.7	1.18

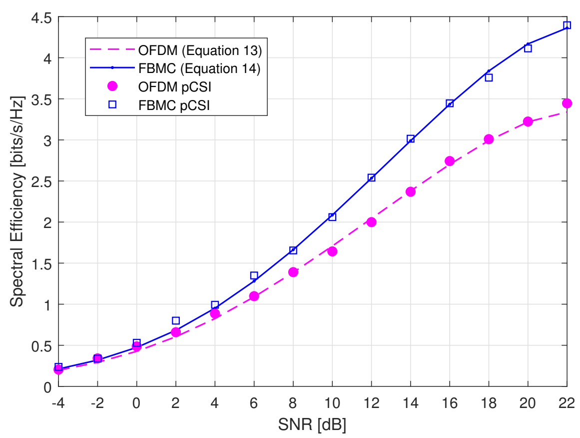

Fig. 3. Comparison between real-world testbed measurements/ Non-Gaussian Modulation and the analytic expressions (13) and (14)

IV. SE for Non-Gaussian Modulations under MM

In order to analyze the spectral properties of different modulation schemes, firstly it is necessary to revisit the expression for SE on a MM system uplink and understand what represents the SNR perceived value for each user. Analyzing equation (2), assuming that $M >> K$ and considering large-scale fading, it is possible to infer that

$$\overline{SNR} = \frac{M-K}{K} \sum_{k=1}^{K} p_u \beta_k \quad (15)$$

where $\overline{SNR}$ is the average SNR perceived per user when a MM system uplink is being evaluated, for ZF signal combination, K users and M antennas. The result of [4] given in (9) leads to a single SNR for all users when power control is presented:

$$SNR_{\lambda_0} = (M-K)\frac{\lambda_0}{\sigma^2}. \quad (16)$$

We recall that λ_0 depends on β of (7), therefore, the SNR in both cases depends on the distance between the BS and the user, the path-loss exponent and the number of users. As shown on (2), p_u is the same for all users, then the SNR per user depends on its individual β_k [3]. To put it differently, the position of the user inside of a cell has great influence on its individual SNR when a MM system uplink is in place. For SNR much higher than 25dB, the modulation SE saturates in 5bits/s/Hz from the 64-QAM (as illustrated on Fig. 1). On the other hand, SNR_{λ_0} is fixed for all users and fall below the saturation of a 64-QAM in our simulations. Thus, the SE expression of (9) is combined with (13) and (14) to derive the cell SE for the OFDM and FBMC modulations, with non-Gaussian distributions on the sub-carriers modulation scheme; which implies that the SE in a MM network and ZF signal combining is represented by:

$$SE_{OFDM-ZF_{cell}} = K \log_2 \left[1 + SNR_{\lambda_0} \left(A_O SNR_{\lambda_0} + B_O \right)^2 \right] \gamma_O \left(A_O SNR_{\lambda_0} + B_O \right), \quad (17)$$

$$SE_{FBMC-ZF_{cell}} = K \log_2 \left[1 + SNR_{\lambda_0} \left(A_F SNR_{\lambda_0} + B_F \right)^2 \right] \gamma_O \left(A_F SNR_{\lambda_0} + B_F \right). \quad (18)$$

V. Simulation

The SE for OFDM and FBMC were analyzed through (17) and (18) considering the parameters from tables I and II. The parameters α, ϕ, r_0, R, σ_{sh}^2, lead to β, which in its turn is used to calculate λ_0, through the equations presented in [4]. The other parameters required for λ_0 are the same that the ones presented in table I of [4]. In order to learn more details about how the ratio λ_0 / σ^2 is calculated it is recommended to review section IV from [4]. By employing the equation (16), it's possible to establish the SNR range used in the simulation. For 25 antennas at the BS and using the parameters on table II, the minimum SNR reached is -0.7 dB. And for 450 antennas at the BS, the maximum SNR reached is 16.4 dB.

On a scenario that considers perfect CSI, Fig. 4 depicts the SE of a MM system uplink when M goes from 25 to

TABLE II
PARAMETERS OF THE MASSIVE MIMO SYSTEM UPLINK

ϕ	α	σ^2	σ^2_{sh}	r_0	R	K	B
1	3.7	-134dBm/Hz	8dB	10m	600m	10	20MHz

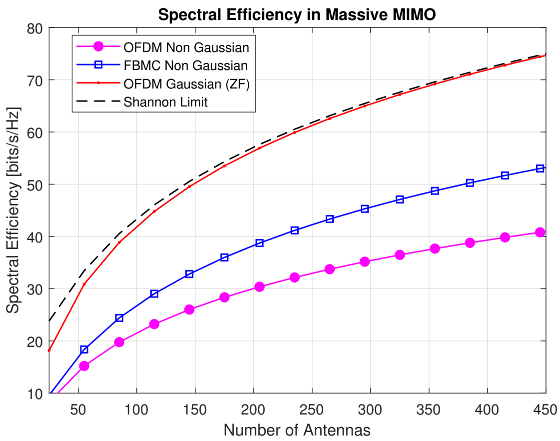

Fig. 4. SE for Gaussian and non-Gaussian modulations in a single cell with radius R=600 m when a ZF detector is placed at the BS.

450 antennas. Fig. 4 shows that the increase of SE is higher at the beginning and the relative difference between SE in OFDM and FBMC increases as N increases. This is expected as the FBMC SE increases faster than the OFDM as the SNR increases, observed from Fig. 1. The FBMC is about 27% better spectral efficiency than OFDM for 150 antennas, and is 33% better for 450 antennas. Another note is that OFDM requires more antennas at the BS to achieve the same SE in bits/s/Hz. For instance, the OFDM SE saturates at 40 bits/s/Hz, needing 450 antennas, more than 2 times than the required for FBMC for the same rate. Both modulated signals are quite far apart from the analytic expressions which considered Gaussian distributed modulations. This shows a more realistic scenario, helping understanding the limits of such MM cells for 5G implementation.

VI. Conclusions

In this article, a way to investigate the SE of a MM system uplink using the throughput data from a SISO signal was introduced. By using this technique, it was possible to compare the SE of OFDM-MQAM and FBMC-OQAM, which is one of the strongest candidates for 5G technology. By assuming a single cell scenario and perfect CSI, it was possible to introduce and analyze the behavior of θ (modulation parameter) extracted from a SISO signal and its relation with the perceived SNR value related to MM, observing that a linear fit was possible and a semi empirical expression was developed for the SE in SISO scenario and non-Gaussian modulations (OFDM and FBMC).

When it comes to the investigation of the SE in a MM setup uplink, it was shown that FBMC-OQAM ensures an improvement of more than 30% over OFDM when $N > 9 \cdot K$. Besides, the saturation point for OFDM and FBMC SE that would be noticed at an SNR above 25dB is not reached in the test bench.

For future studies, a range of different Massive MIMO scenarios could be analyzed, such as systems using Rician or Nakagami-m fading instead of Rayleigh and also, the usage of millimeter waves. Those assumptions could provide a better understanding of the real potential of OFDM and FBMC as candidates to address some of the 5G requirements to deliver high-speed data transfer rates and more reliable services.

References

[1] A. J. PAULRAJ, D. A. GORE, R. U. NABAR, and H. BOLCSKEI, “An overview of mimo communications - a key to gigabit wireless,” *Proceedings of the IEEE*, vol. 92, no. 2, pp. 198–218, Feb 2004.
[2] J. G. Andrews, S. Buzzi, W. Choi, S. V. Hanly, A. Lozano, A. C. K. Soong, and J. C. Zhang, “What will 5g be?” *IEEE Journal on Selected Areas in Communications*, vol. 32, no. 6, pp. 1065–1082, June 2014.
[3] H. Q. Ngo, E. G. Larsson, and T. L. Marzetta, “Energy and spectral efficiency of very large multiuser mimo systems,” *IEEE Transactions on Communications*, vol. 61, no. 4, pp. 1436–1449, April 2013.
[4] L. Zhao, K. Li, K. Zheng, and M. O. Ahmad, “An analysis of the tradeoff between the energy and spectrum efficiencies in an uplink massive mimo-ofdm system,” *IEEE Transactions on Circuits and Systems II: Express Briefs*, vol. 62, no. 3, pp. 291–295, March 2015.
[5] C. He, B. Sheng, P. Zhu, X. You, and G. Y. Li, “Energy- and spectral-efficiency tradeoff for distributed antenna systems with proportional fairness,” *IEEE Journal on Selected Areas in Communications*, vol. 31, no. 5, pp. 894–902, May 2013.
[6] C. E. Shannon, “A mathematical theory of communication,” *The Bell System Technical Journal*, vol. 27, no. 4, pp. 623–656, Oct 1948.
[7] A. Farhang, N. Marchetti, F. Figueiredo, and J. P. Miranda, “Massive mimo and waveform design for 5th generation wireless communication systems,” in *1st International Conference on 5G for Ubiquitous Connectivity*, Nov 2014, pp. 70–75.
[8] J. Vihriala, N. Ermolova, E. Lahetkangas, O. Tirkkonen, and K. Pajukoski, “On the waveforms for 5g mobile broadband communications,” in *2015 IEEE 81st Vehicular Technology Conference (VTC Spring)*, May 2015, pp. 1–5.
[9] F. Schaich and T. Wild, “Waveform contenders for 5g x2014; ofdm vs. fbmc vs. ufmc,” in *2014 6th International Symposium on Communications, Control and Signal Processing (ISCCSP)*, May 2014, pp. 457–460.
[10] R. Nissel, S. Schwarz, and M. Rupp, “Filter bank multicarrier modulation schemes for future mobile communications,” *IEEE Journal on Selected Areas in Communications*, vol. 35, no. 8, pp. 1768–1782, Aug 2017.
[11] T. L. Marzetta, “Massive mimo: An introduction,” *Bell Labs Technical Journal*, vol. 20, pp. 11–22, 2015.
[12] K. N. R. S. V. Prasad, E. Hossain, and V. K. Bhargava, “Energy efficiency in massive mimo-based 5g networks: Opportunities and challenges,” *IEEE Wireless Communications*, vol. 24, no. 3, pp. 86–94, June 2017.
[13] E. G. Larsson, O. Edfors, F. Tufvesson, and T. L. Marzetta, “Massive mimo for next generation wireless systems,” *IEEE Communications Magazine*, vol. 52, no. 2, pp. 186–195, February 2014.
[14] R. Nissel and M. Rupp, “Ofdm and fbmc-oqam in doubly-selective channels: Calculating the bit error probability,” *IEEE Communications Letters*, vol. 21, no. 6, pp. 1297–1300, June 2017.
[15] P. Sabeti, A. Farhang, N. Marchetti, and L. Doyle, “Performance analysis of fbmc-pam in massive mimo,” in *2016 IEEE Globecom Workshops (GC Wkshps)*, Dec 2016, pp. 1–7.
[16] A. Farhang, N. Marchetti, L. E. Doyle, and B. Farhang-Boroujeny, “Filter bank multicarrier for massive mimo,” in *2014 IEEE 80th Vehicular Technology Conference (VTC2014-Fall)*, Sept 2014, pp. 1–7.
[17] F. Schaich, “Filterbank based multi carrier transmission (fbmc) x2014; evolving ofdm: Fbmc in the context of wimax,” in *2010 European Wireless Conference (EW)*, April 2010, pp. 1051–1058.
[18] D. Zhang, M. Matthé, L. L. Mendes, and G. Fettweis, “A study on the link level performance of advanced multicarrier waveforms under mimo wireless communication channels,” *IEEE Transactions on Wireless Communications*, vol. 16, no. 4, pp. 2350–2365, April 2017.